Surface electronic structure of two- and three-dimensional holmium silicide on Si(111)

Charles Woffinden, Christopher Eames, Hervé Ménard, and Steve P. Tear
Department of Physics, University of York, York YO10 5DD, United Kingdom

Andrew Pratt*
Department of Physics, York Institute for Materials Research, University of York, York YO10 5DD, United Kingdom
(Received 6 February 2009; revised manuscript received 5 May 2009; published 5 June 2009)

The surface electronic structure of two- and three-dimensional Ho silicides grown on Si(111) has been studied with the techniques of metastable de-excitation spectroscopy (MDS) and ultraviolet photoemission spectroscopy. Electronic structure differences between the two cases are examined, and the extreme sensitivity of MDS to the surface density of states (DOS) allows a direct comparison between deconvolved spectra and *ab initio* density-functional theory calculations. This comparison shows a good agreement between the DOS calculated for the Si(111)-1×1-Ho structure and MDS data obtained from an almost-complete layer of two-dimensional Ho silicide. The dominant role of the topmost silicon bilayer in determining the surface electronic properties is revealed.

DOI: 10.1103/PhysRevB.79.245406 PACS number(s): 73.20.−r, 73.21.−b, 71.15.Mb

I. INTRODUCTION

Rare-earth (RE) silicide growth on semiconductor substrates shows promise as a metal/semiconductor interface for a number of materials systems including nanowires,[1] RE silicide heterostructures,[2] and high-k dielectrics for complementary metal-oxide semiconductor (CMOS) devices.[3] Applications utilizing the low Schottky barriers [0.3–0.4 eV for n-type Si(111)] of these systems, such as metal-oxide-semiconductor field-effect transistors (MOSFETs) (Ref. 4) and infrared sensors,[5] have also been demonstrated. Despite this activity the growth of REs on Si is still not fully understood; however obtaining high-quality interfaces is essential as their atomic structure in turn determines their electronic properties. To this end we have conducted an electronic study of the formation of $HoSi_{2-x}$ on Si(111), where $x=0$ for the two-dimensional (2D) silicide and $x\approx0.3$ for the three-dimensional (3D) silicide.

The atomic and electronic structures of both 2D and 3D RE silicides on Si(111) have been studied with a number of techniques including medium-energy ion scattering (MEIS),[6,7] low-energy electron diffraction (LEED),[8,9] scanning tunneling microscopy (STM),[10,11] Auger and photoelectron diffraction,[12] and surface x-ray diffraction (SXRD).[13] This research has revealed strong similarities in the structure formed when different trivalent RE metals (e.g., Dy, Ho, and Er) are deposited on Si(111) and the structural models deducted are shown in Fig. 1. For a 2D RE silicide [Fig. 1(a)], RE atoms are positioned in the $T4$ sites of the substrate Si forming a single layer, above which sits a buckled Si bilayer of opposite buckling direction to the bulk (type B buckling, as opposed to type A buckling in which atomic positions mirror those of the bulk-terminated surface). The reverse buckling occurs as the configuration of Si atoms results in the maximum number of nearest neighbors for each RE atom therefore stabilizing the structure. Among the three valence electrons of the trivalent REs available for bonding, two directly bond to the upward- and downward-pointing dangling bonds (DBs) of the substrate and surface bilayer Si atoms, respectively, forming a saturated closed-shell structure.[14] A third, via charge transfer, partially compensates the outward-pointing DBs of the top Si atomic layer. The resulting surface displays a $p(1\times1)$ periodicity and is relatively passive, making it a good candidate for further growth studies.

For increased deposition of a RE metal a 3D silicide forms, which is similar to the 2D case except with alternating flat layers of RE and graphitelike Si between the substrate and the surface [Fig. 1(b)] which may display either a B-type buckling or a combination of both A- and B-type bucklings. To relieve strain, an ordered network of vacancies is distributed throughout the flat Si layers, with one missing for every six Si atoms, giving rise to a $RESi_{1.7}$ stoichiometry and a $(\sqrt{3}\times\sqrt{3})R30°$ LEED pattern. The vacancy network has been proposed as a reason for the mixing of buckling types at the surface where the buckling itself relieves strain so that no vacancies exist here. STM studies have shown $(\sqrt{3}\times\sqrt{3})R30°$ modulations in the surface bilayer of the 3D reconstruction which have been suggested to arise due to the underlying vacancies, although the details are disputed and vacancy periodicities of $1c$, $2c$, and $3c$ have all been reported.[15–18]

Among the techniques used to investigate the electronic structure of 2D and 3D RE silcides, ultraviolet photoemission spectroscopy (UPS) has been the most revealing, especially when its results are compared to theoretical calculations. However, photons penetrate below the surface to some degree so that information regarding the outermost electronic structure contains a significant contribution from the bulk. A complementary technique to UPS which also probes surface valence-band states is metastable de-excitation spectroscopy (MDS) which measures the ejected electron-energy spectrum emitted from a sample due to the de-excitation of metastable rare-gas atoms (usually the 2^3S state of He). As the cross section for de-excitation is so large, this process occurs several Å from the sample rendering MDS an extremely sensitive probe of the outermost surface electronic structure. We have used MDS and UPS to investigate the differences between the surface electronic structure of 2D and 3D RE silicides. The dynamics of the de-excitation process in MDS results in spectra that are essentially a reflection of the self-

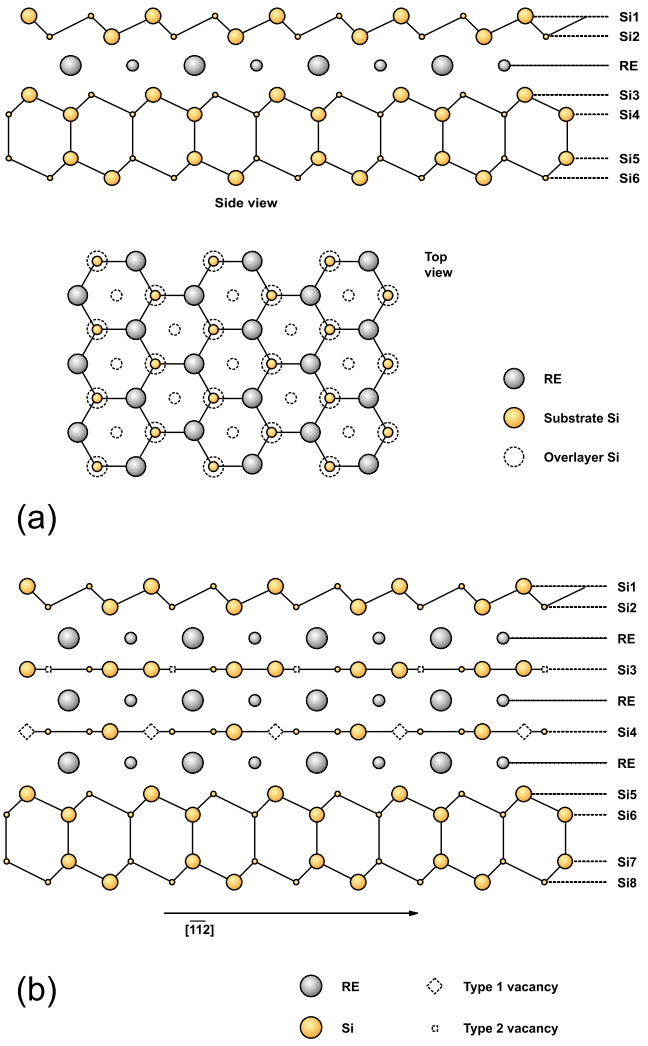

FIG. 1. (Color online) A structural model of *B*-type buckled (a) 2D and (b) 3D RE silicides.

convolved surface density of states (SDOS). To enable a direct comparison with *ab initio* density-functional theory (DFT) calculations, the MDS spectra are deconvolved.

The first theoretical calculation involving RE silicides on Si(111) was by Stauffer *et al.*[14] in 1993 who used a semiempirical technique to determine the band structure for a variety of top-layer orientations in 2D Si(111)-1 × 1-Er. Although they did not geometry optimize the system, they showed that the reverse-buckled top layer gives the best match with the experimentally obtained band structure. In 2004 Rogero *et al.*[19] extended this work using DFT to show that the electronic structure of $ErSi_2$ was common to all the trivalent RE silicides. They did this by showing a favorable comparison of DFT simulations of the density of states (DOS) and the band structure for 2D Si(111)-1 × 1-Y and 2D Si(111)-1 × 1-Gd with the results of angle-resolved ultraviolet photoemission spectroscopy (ARUPS) experiments and with previous theoretical work. They provided a full analysis of the electronic structure in the 2D RE silicides using charge density and charge-density difference plots and layer-resolved DOS curves.

The atomic structure has received similar theoretical attention. Rogero *et al.*[8] used the SIESTA code to geometry optimize the 2D Si(111)-1 × 1-*Y* structure and found a good level of agreement with the structural parameters obtained by LEED. Cocoletzi *et al.*[20] slightly improved these structural parameters and performed the first DFT simulations of a 3D silicide surface, including a detailed investigation of the energetics of the networks of Si vacancies in the graphitic Si layers. The first DFT calculation was that of Magaud *et al.*[21] To help understand the role of the vacancy network in the 3D silicides they looked at the bulk-hexagonal silicide structure formed by the group III RE metal Y, with the choice of RE metal atom being due to the lack of *f* electrons in Y and the computational savings to be made therein. Comparison of theoretically generated STM images with experiment was first carried out by Duverger *et al.*[10] to explain the bias-voltage dependence of the STM images for 2D and 3D silicides. Later simulated STM work by Rogero *et al.*[18] showed the influence of the vacancy network within the 3D silicide upon the structure of the top bilayer and demonstrated that two different subsurface vacancy networks can coexist. The picture was further enriched by Peng *et al.*[22] who showed using the nudged elastic band method that there is very prominent Si diffusion within the defect-rich graphitic Si layers. The DFT calculations in Sec. II of this work concentrate on the top silicon bilayer and have two principal aims: (1) provide theoretical support for the surface bilayer sensitive MDS data and (2) show the importance of temperature in determining the structure of the top layer.

II. *AB INITIO* STUDY OF 2D HOLMIUM SILICIDE

We have used the CASTEP code[23] to geometry optimize our structures and to calculate their electronic properties. The code was run in a parallel computing environment on a Beowulf cluster of 33 machines, each with dual Intel Pentium 4 Xeon processors running at 1.7 GHz in the Department of Physics at York. A typical geometry optimization calculation used 18 processors and required around 200 h.

Ensemble DFT was used to improve the convergence of the electronic structure calculation (this is of particular use in a system that contains a RE metal atom). The Perdew-Burke-Ernzerhof[24] generalized gradient approximation was used to represent exchange and correlation effects. We have used ultrasoft pseudopotentials, and for complete accuracy we have included all frequency components of the wave functions in the construction of the soft charge density from the calculated wave functions. We have also converged our supercells with respect to the augmentation charge-density sampling grid.

Before proceeding with the geometry optimization the input parameters were carefully checked. The variation in the calculated energy with the number of plane waves included in the calculation shows that a cutoff energy of 400 eV yields a total energy near the variational minimum and will allow accurate calculation of the energy and the forces within the system. At a given cutoff energy the total energy was then calculated for three increasingly dense Monkhorst-Pack[25] reciprocal-space sampling grids. A reciprocal-space sampling grid with 18 *k* points was used in the geometry optimization since increasing the sampling grid size to 32 *k* points does not significantly change the energy.

TABLE I. Layer spacings in the Si(111)-1×1-Ho system determined by DFT in this work compared with the results from other experimental studies. Those parameters marked with an asterisk have not been optimized. Spacings are defined in Fig. 1.

	LEED (Ref. 26)	MEIS (Ref. 27)	DFT
Si1-Si2 (Å)	0.82	0.88 ± 0.03	0.64
Si2-Ho (Å)	1.88	1.83 ± 0.03	1.89
Ho-Si4 (Å)	2.03	2.10 ± 0.06	2.01
Si4-Si5 (Å)	1.01	0.90 ± 0.06	0.89
Si5-Si6 (Å)	2.305	2.245*	2.31
Si6-Si7 (Å)	0.78	0.78*	0.72

The vacuum gap must be of sufficient thickness to prevent interaction between the top surface in one supercell and the bottom surface in the supercell above. For a fixed atomic geometry and basis set the energy and the mean force on all of the atoms in the supercell were calculated as a function of the thickness of the vacuum gap. A vacuum gap of 9 Å or above is sufficient to minimize interactions across this expanse. We have found four bulklike silicon layers sufficient to minimize interactions through the supercell between uncompensated charges in the top and bottom layers. The bottom bulklike silicon layer has been hydrogen passivated to quench dangling bonds and to reduce the number of layers needed in the slab (this also reduces the thickness of the vacuum gap that is needed).

The Si(111)-1×1-Ho system was geometry optimized using the structure suggested by LEED as an initial atomic configuration.[26] The structural parameters are compared to the experiment in Table I below, and we can see that there is reasonable agreement. The structure was allowed to relax until the forces were below the predefined tolerance of 5×10^{-2} eV Å^{-1}.

We can see that the main difference between experiment and theory is in the rumpling amplitude of the top Si bilayer. The structure suggested by DFT is at 0 K, and the effect of temperature upon the surface reconstruction is not included. However, there is much experimental evidence to suggest that the vibrations of the top silicon bilayer are markedly greater than in the silicon bulk. Indeed, Rogero *et al.* reported significant improvement in the Pendry *R* factor obtained in a LEED *I-V* structure fit for Y-Si(111)-1×1 if the vibrational amplitudes of each layer are individually optimized. Clearly, then, temperature plays a dominant role in the vertical spacings within this system and in the related 2D silicides.

The means of comparison with experiment in this work is through the SDOS. The extreme sensitivity of MDS to the top exposed layer and any orbitals that protrude through this from any layers below or any bulk states means that we can use the atomically resolved DOS suggested by DFT to assign features in the deconvolved MDS spectrum to individual atoms. To evaluate the partial DOS from the calculated band structure we have used an interpolation method with an instrumental broadening function applied. It was found that a 6×6×6 *k*-point sampling mesh was required to converge the DOS. To resolve the DOS by atom or by angular-momentum channel [partial density of states (PDOS)], the Mulliken population analysis is used which determines the contribution from each energy band to a given atomic orbital.

III. EXPERIMENT

All preparation and measurements were conducted within the same vacuum chamber equipped with LEED, UPS, and MDS under ultrahigh vacuum with a typical base pressure of approximately 3×10^{-10} mbar. The MDS experimental setup has been described in detail elsewhere.[28] In short, a beam of metastable (2^3S) He atoms is produced in a hollow cold-cathode dc discharge source. This supersonically expands into a chamber, where laser cooling, using light tuned to the He 2^3S_1-2^3P_2 transition at 1083 nm, is used to collimate the beam along the He beamline axis. This collimation process increases both the intensity and purity of the He 2^3S beam, as neither UV photons nor 2^1S He atoms produced in the source are collimated and so continue to diverge. This leads to a He 2^3S intensity of the order of 10^{12} atoms s^{-1} cm^{-2} at the sample. From here, the beam enters the analysis chamber and impinges on the sample at 45° to the surface normal.

For UPS experiments, He I resonance photons ($h\nu$ =21.22 eV) were produced from a He discharge and were again incident on the sample at 45° to the surface normal. The electron energy spectra for both MDS and UPS were measured at normal emission by an Omicron Vakuumphysik GmbH EA125 hemispherical analyzer.

Si(111) samples were cut from a lightly doped *n*-type wafer. These were outgassed for approximately 8 h at 400 °C and subsequently cleaned by direct current heating to approximately 1200 °C as measured on an infrared pyrometer for 1 min, followed by a gradual cool to room temperature. This cleaning process was repeated at least three times until the LEED pattern showed sharp spots indicating a 7×7 reconstruction.

Holmium deposition was achieved by the direct current heating of a Ta boat containing a Ho ingot and deposition rates were calibrated using a quartz-crystal oscillator. During deposition, the chamber pressure did not rise above 5×10^{-10} mbar. The sample was held at room temperature during deposition and was subsequently annealed for 10 min at approximately 500 °C to achieve the silicide structure. In this paper the coverages quoted are nominal but in reality the local-film thicknesses may differ from these values due to islanding in some regions of the surface.

After preparation, LEED patterns were checked for all samples to ensure that a good surface reconstruction had been achieved. The 2D silicide surface exhibited a bright, threefold, $p(1\times1)$ LEED pattern as would be expected. The 3D silicide surfaces all gave a $(\sqrt{3}\times\sqrt{3})R30°$ LEED pattern with the less common threefold (as opposed to sixfold) rotational symmetry. A threefold pattern suggests that the surface is well ordered so that the bilayer buckling is either all *A* type or all *B* type. A sixfold pattern would indicate an equal presence of both domains of buckling over the surface. The $(\sqrt{3}\times\sqrt{3})$ LEED spots arise due to the presence of vacancies in the graphitelike Si layers (see Fig. 1). The LEED pattern for the 2 ML coverage exhibits weak $(\sqrt{3}\times\sqrt{3})R30°$, spots

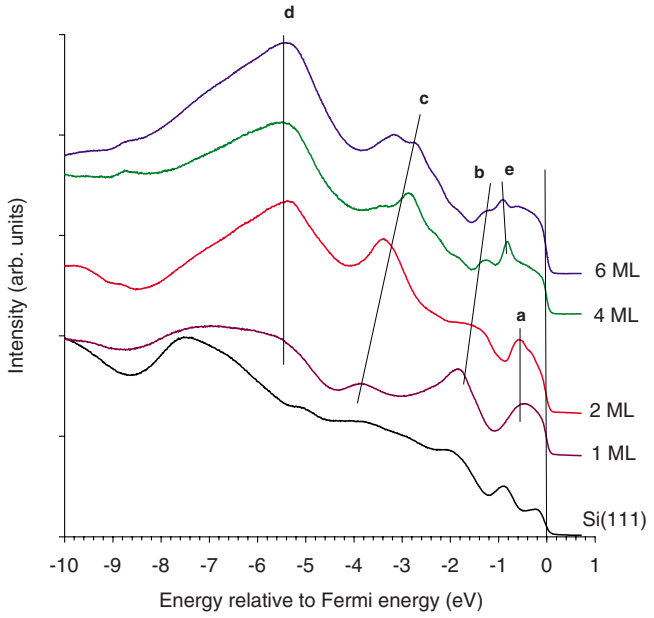

FIG. 2. (Color online) UPS spectra for various $HoSi_{2-x}$ coverages on Si(111). The Si(111) spectrum is provided for reference. The spectra are offset for clarity.

indicating that the surface probably consists of a combination of 2D silicide and 3D islands. In our case, for the 3D silicide, the orientation of the LEED spots was the same as for the 2D silicide which indicates a *B*-type buckled surface. In this study, 1, 2, 4, and 6 ML films were grown and investigated. MDS and UPS experiments were then conducted on the clean silicide surfaces.

IV. RESULTS AND DISCUSSION

A. UPS

The UPS spectra for surfaces of Si(111) with different coverages of Ho are presented in Fig. 2. Marked contrasts appear with increasing coverage, particularly among the 1, 2, and 4 ML silicide surfaces. The spectrum for clean Si(111) 7×7 is provided for reference.

The clean Si spectrum shows peaks characteristic of the 7×7 reconstruction surface states at −0.2 and −0.9 eV from dangling bonds and at −2.0 eV from backbond states.[29,30] These peaks are suppressed after Ho silicide formation, as would be expected when a new surface reconstruction forms.

A previous UPS study has been conducted for 2D and 3D $ErSi_{2-x}$ which highlighted similar features to the ones presented in this paper.[31] In the 1 ML spectrum, the peak labeled as a is thought to be a superposition of two features: both a Si surface feature and a Ho feature. The surface feature previously noted by Saintenoy *et al.*[31] at −0.1 eV relative to E_F has been explained as a Si surface state from p_z dangling bonds. A large emission is also expected to arise from the Ho $5d$ emission at E_F. The peak labeled as b is thought to result from another surface state with the p_z character derived from the dangling bonds of Si atoms.[14,32] It may also have some contribution from the Si backbond state from any remaining, exposed Si(111). Feature c has been attributed to an electronic state from the hybridized RE $5d$ and Si $3p$ electrons. With an increased Ho coverage, this feature increases in intensity supporting this at least partial Ho origin. The much broader peak at d is due to the corelike RE $4f$ states and is therefore not involved in the silicide bonding structure and would therefore not appear in the MDS spectrum.[31–33]

A slight change in the spectra for the 3D silicides is expected due to the presence of vacancies within the structure, slightly modifying the DOS. For the 3D silicides, some of the features, such as c and d, are similar to the 1 ML case, although some relocate slightly in energy as a result of the changes in crystal potential. For the 2 ML coverage, the features are all at very similar energies to the 1 ML case. The feature labeled as b, earlier attributed to Si dangling bonds, has decreased in intensity. As the coverage increases, the peak labeled as a in the 2D case splits into a shoulder and separate peak, labeled as e, in the 3D case. The shoulder is likely due to the p_z electronic states mentioned previously. This peak at 0.9 eV is similar in energy to a feature noted by Saintenoy *et al.* resulting from the $3p_z$ electrons in vacancies.[31] This would explain its absence from the 2D spectra.

B. MDS

When MDS is performed on metallic, semimetallic, and low band gap semiconducting surfaces such as the ones studied in this paper, the de-excitation process that takes place is predominantly resonance ionization (RI) followed by Auger neutralization (AN). This is the case for the Si(111) surface. Initially, the 2^3S atoms are resonantly ionized, where the He $2s$ electrons tunnel into an empty surface state, thus leaving a He^+ ion which continues to approach the surface. Auger neutralization follows, where a surface electron transfers into the He^+ ground state, simultaneously liberating another surface electron in an Auger-type transition. As RI+AN is a two-electron process, the bands in the SDOS are self-convolved, and so the resulting spectra lack sharp features. For insulating surfaces and high band gap semiconductors, the de-excitation mechanism that occurs is Auger de-excitation. In this process, an electron tunnels from the surface to fill the $1s$ vacancy. The $2s$ electron is simultaneously liberated. In both these de-excitation processes, as the He 2^3S interacts with the orbitals furthest into the vacuum, the technique is extremely sensitive to the SDOS.

The MDS spectra acquired at room temperature are presented in Fig. 3 for the same coverages as for UPS. These spectra have been normalized to the maximum of the 4 ML spectrum so that relative intensities can be directly compared. As the maximum emission occurs at an energy where bulk states dominate, this should not unfairly bias the magnitude from the surface states.

The MDS spectrum for the clean Si(111)-7×7 surface displays three distinct features: a peak and two shoulders. The peak, centered at 8.5 eV, is due to $3p$ electrons from the bulk states.[34] The shoulder at around 10.3 eV has not previously been reported in MDS spectra but a peak at approximately 3.0 eV below E_F in the SDOS has been predicted by tight-binding theory calculations arising from surface dimer

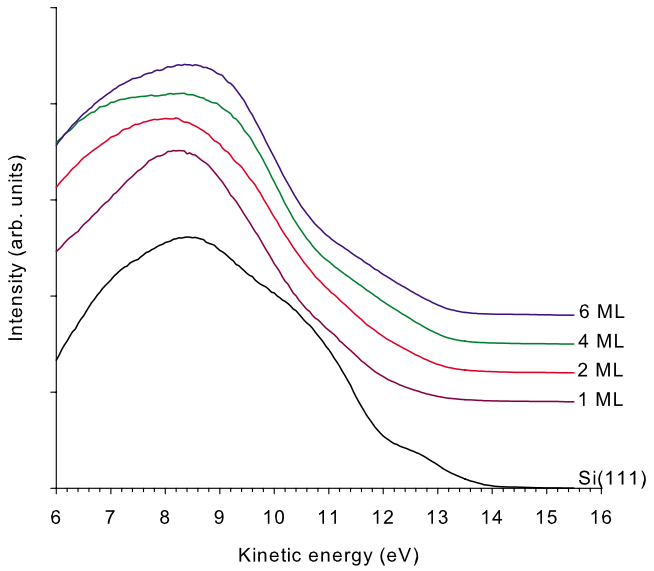

FIG. 3. (Color online) MDS spectra for various $HoSi_{2-x}$ coverages on Si(111). Spectra have been offset on the intensity axis for clarity.

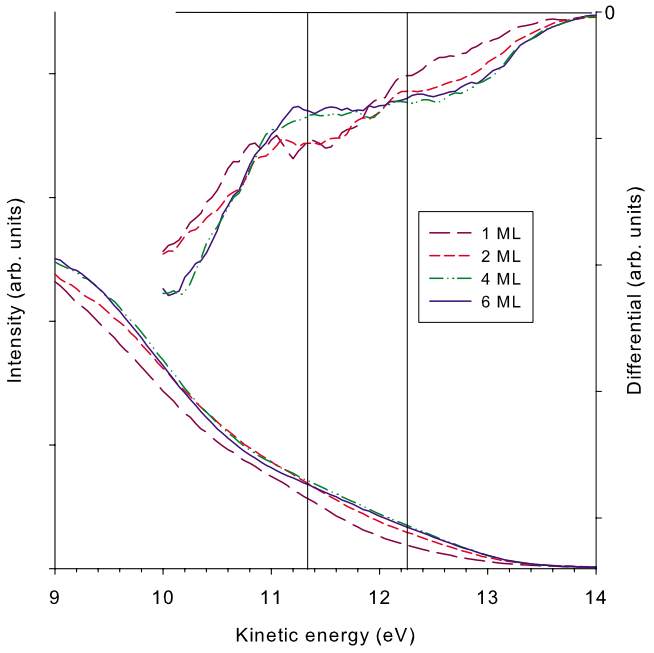

FIG. 4. (Color online) MDS spectra for various $HoSi_{2-x}$ coverages on Si(111). The right-hand axis shows the first differentials of the spectra. Differentiated spectra have been smoothed.

states.[35] This corresponds to the energy at which the shoulder is observed in the MDS spectrum. The suggestion of the feature's origin is further supported by the fact that it disappears completely with even small coverages of Ho, indicating that it is indeed the result of a surface state of the 7×7 surface. The smaller shoulder at 12.7 eV has been much studied[34,36] and is due to the same surface-state backbonds and dangling bonds as seen in the UPS spectrum, but with MDS they are convolved into the same feature. The de-excitation process that occurs for the Ho silicide samples is also RI+AN, providing further evidence for its semimetallic properties.[14] The main peak in all the 2D and 3D Ho silicide spectra is due to the Si $3p$ bulk states as in the case of Ho on Si(100) and the clean Si(111)-7×7 surface.[33,34] A slight difference is apparent between the 2D and 3D surfaces in the higher-energy tails of the spectra (approximately 11–14 eV), where emission due to surface states is expected. This region is shown in more detail in Fig. 4. To emphasize the subtle differences between the spectra, the differentiated spectra are also presented.

The energy range over which the differences occur correspond to the region with a high p-state contribution in the DFT predicted SDOS. As the He 2^3S de-excitation is sensitive only to the outermost orbitals of the surface, and this feature is at a relatively high energy, this indicates a difference in the electronic structure of the top-buckled Si layer.

V. DECONVOLVED MDS SPECTRA COMPARED WITH DENSITY-FUNCTIONAL THEORY DOS

As MDS gives a self-convolved spectrum, it is possible to deconvolve this spectra in order to achieve an estimate of the SDOS modified by the transition probability of the de-excitation process.[37] $P(\varepsilon)$, the transition probability (effectively the self-convolved MDS spectrum), is given by the self-folded integral,

$$P(\varepsilon) \propto \int_{-\varepsilon}^{\varepsilon} U(\varepsilon-\Delta\varepsilon)U(\varepsilon+\Delta\varepsilon)d(\Delta\varepsilon),$$

where $U(\varepsilon)$ is the transition density for an electron in the surface, i.e., the local DOS modified by the transition probability.[37] ε is the mean binding energy of the electrons involved in the transition relative to E_F. This expression can be solved for $U(\varepsilon)$ providing us with an effective deconvolved signal. This has been done for the $HoSi_{2-x}$ using similar methods to Ishii *et al.*[37] The DFT calculated SDOS is presented alongside experimental results to allow a direct comparison in Fig. 5.

With the self-convolved spectra, one cannot know from what binding energy an electron originates, but as the spectra are now deconvolved, the energy scale can be converted to the binding energy of the electron. The deconvolution of the 1 ML spectrum shows poor agreement with the theoretical prediction. However, it is known that a nominal 1 ML coverage does not form a uniform 2D coverage[38] as can be seen in Fig. 6. Gaps in the 2D silicide are apparent, revealing unexposed Si underneath. A few 3D islands are also visible. In comparison, the 2 ML nominal coverage film has a much more uniform 2D coverage with some islands of 3D Ho evident on top of this. These islands are all of very similar height at (5.3 ± 0.5) Å above the 2D film and have an average full width at half maximum (FWHM) diameter of (12 ± 3) nm. Between the islands, the film of 2D Ho silicide is almost completely unbroken.

The 2 ML deconvolution shows the best agreement to the DFT, again supporting the view that the 2 ML coverage exhibits predominantly 2D behavior. This growth pattern has been observed extensively within the group using STM when growing 2 ML films in this fashion. For thicker coverages,

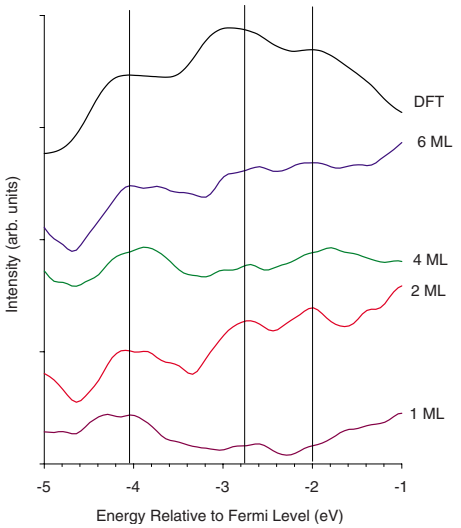

FIG. 5. (Color online) Deconvolution of MDS spectra for various Ho silicide coverages on Si(111) compared to density of states calculated by DFT for the 2D $HoSi_2$ surface. Deconvolved spectra have been smoothed and offset for clarity.

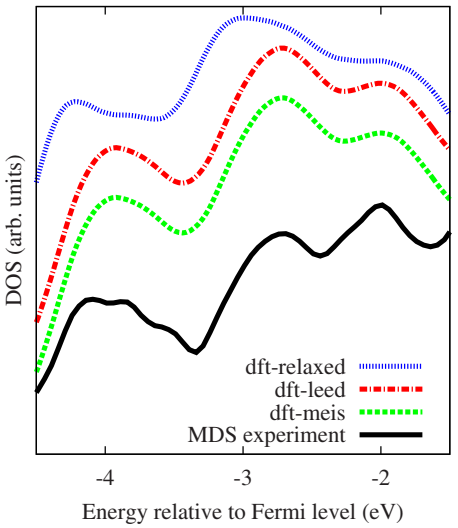

FIG. 7. (Color online) Deconvolved MDS data for a continuous layer of 2D $HoSi_2$ on Si(111) compared to the DOS calculated for three different structures suggested by MEIS, LEED, and 0 K DFT. Data have been offset for clarity.

the 4 and 6 ML also have reasonable agreement to the DFT, especially with the complete unit-cell DOS model. The three features from the DFT are still apparent but are less intense than for the 2 ML surface. This suggests that the SDOS is slightly altered between the 2D and the 3D surfaces. This may be an effect of a change in the rumpling amplitude or could result from a modification in the spacing between the Si2 layer and Ho layer.[7,39]

Figure 7 shows the 2 ML MDS data with theoretical DOS calculated for three different structures: that suggested by MEIS, that suggested by LEED, and the geometry optimized DFT structure which was obtained in Table I. It is clear that the structure models derived from experimental fitting techniques produce calculated DOS that are much closer to experimental DOS obtained from MDS than that from the DFT optimized structure. This shows the effect of finite temperature on the structure. DFT relaxation of the structure should, therefore, be done at room temperature and perhaps calculations using molecular dynamics would be of use. The sensitivity of the DOS to the atomic structure of the topmost two layers reveals how much the electronic structure depends on the temperature at which the measurements were made in this case.

It is possible to resolve the features in the MDS spectrum using the DFT PDOS analysis. Figure 8 shows a layer-by-layer decomposition of the DOS for the structure suggested by MEIS. The layers were defined in Fig. 1. There is a significant contribution from layers below the top bilayer. The peak at −4.1 eV appears to entirely represent the silicon bulk

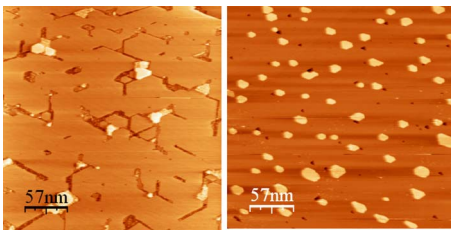

FIG. 6. (Color online) STM image showing incomplete silicide coverage in a 1 ML film of $HoSi_{2-x}$ on Si(111) (left). At higher coverages as 3D silicide islands start to form the silicide layer is complete (right). Thus a 2 ML film can be considered as a better comparison to an infinitely periodic and defect-free DFT supercell than a 1 ML coverage.

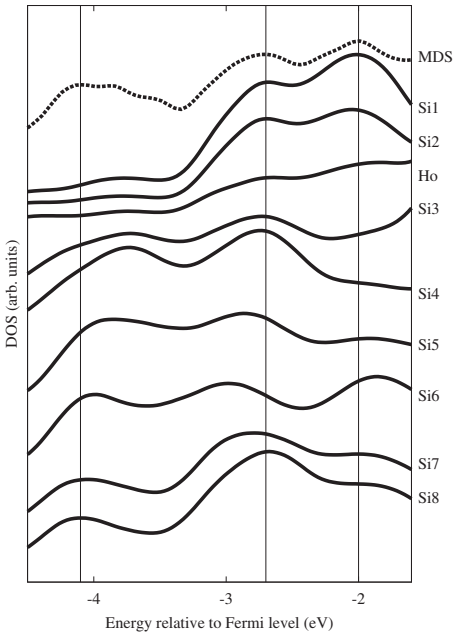

FIG. 8. Layer-resolved partial DOS from DFT compared with the deconvolved MDS experimental data. Bulk states appear to be responsible for the lower-energy peak at −4.1 eV and the peaks at −2.0 and −2.7 eV appear most sensitive to the top bilayer. The structure used in the calculation was that suggested by MEIS. The layers are shown in Fig. 1.

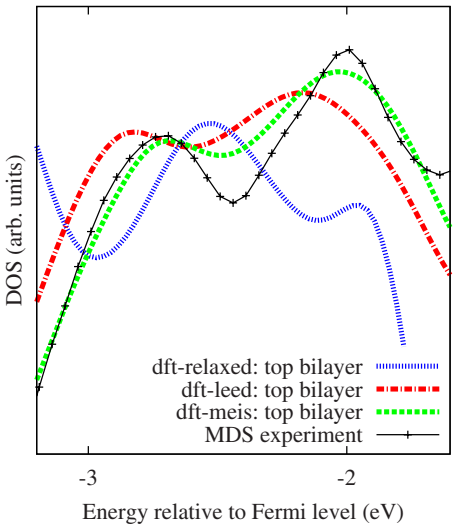

FIG. 9. (Color online) Deconvolved MDS data for a continuous layer of 2D $HoSi_2$ on Si(111) compared to the DOS calculated for the top Si bilayer for three different structures suggested by MEIS, LEED, and 0 K DFT (Table I).

layers below the rare-earth layer or exposed bulklike silicon elsewhere on the surface. The peak at −2.7 eV is sensitive to the top bilayer but has a contribution from the silicon bilayer immediately below the rare-earth layer. The peak at −2.0 eV, however, appears to be exclusively sensitive to the very top silicon bilayer and is therefore the only feature in the spectrum that is exclusively sensitive to the exposed surface layer.

Figure 9 shows the calculated DOS for the top silicon bilayer only (layers Si1 and Si2 in Fig. 1) for the structures suggested by the three techniques as compared to the experimental data near the surface-bilayer sensitive peaks. The MEIS structure model gives the best agreement. This is to be expected since in MEIS the positions of the surface bilayer are readily determined directly from the data. In LEED, however, the part of the data directly corresponding to the top bilayer cannot be isolated from the *I-V* curves and separately fitted to high accuracy without simultaneously fitting the structure of subsurface layers.

VI. CONCLUSIONS

Using a combination of MDS and UPS, the surface electronic structures of 2D $HoSi_2$ and 3D $HoSi_{2-x}$ on Si(111) have been compared and found to differ subtly. This could well be the result of a small change in the buckled Si surface rumpling or the layer spacing between the Ho and buckled Si bilayer.

Deconvolution of the MDS spectra has been conducted to retrieve the effective surface density of states which has then been compared with the DFT predicted density of states to reveal a good agreement between the two for an unbroken 2D film. These deconvolved experimental spectra again reveal a subtle difference between the density of states of the 2D and 3D silicide surfaces.

The deconvolved spectra have been compared to the surface density of states predicted by the DFT for a variety of structural models. From these, it is found that the experimentally determined structure models show better agreement with the MDS data than 0 K structural-relaxation models. This supports previous studies that have shown the important effect of temperature upon the 2D structure of the silicides,[8,40] and since the significant difference arises in the top bilayer buckling, this indicates the high surface sensitivity of MDS. Layer-resolved predicted density of states calculations suggest that the subtle difference in the MDS spectra for the 2D and 3D reconstructions arises from the top few atomic layers in the surface which again provides an evidence for a modification of the surface structure between the two reconstructions.

ACKNOWLEDGMENT

We would like to acknowledge the UK Engineering and Physical Sciences Research Council for funding this project.

*spt1@york.ac.uk

[1] D. R. Bowler, J. Phys.: Condens. Matter **16**, R721 (2004).
[2] Y.-L. Jiang, Q. Xie, C. Detavernier, R. V. Meirhaeghe, G.-P. Ru, X.-P. Qu, and B.-Z. Li, J. Appl. Phys. **102**, 033508 (2007).
[3] O. Engström, B. Raeissi, S. Hall, O. Buiu, M. Lemme, H. Gottlob, P. Hurley, and K. Cherkaoui, Solid-State Electron. **51**, 622 (2007).
[4] S. Zhu, J. Chen, M. Li, S. Lee, J. Singh, C. Zhu, A. Du, C. Tung, A. Chin, and D. Kwong, IEEE Electron Device Lett. **25**, 565 (2004).
[5] L. Pahun, Y. Campidelli, F. A. d'Avitaya, and P. A. Badoz, Appl. Phys. Lett. **60**, 1166 (1992).
[6] T. J. Wood, C. Bonet, T. C. Q. Noakes, P. Bailey, and S. P. Tear, Surf. Sci. **598**, 120 (2005).
[7] T. J. Wood, C. Bonet, T. C. Q. Noakes, P. Bailey, and S. P. Tear, Phys. Rev. B **73**, 235405 (2006).
[8] C. Rogero, C. Polop, L. Magaud, J. L. Sacedon, P. L. de Andres, and J. A. Martín-Gago, Phys. Rev. B **66**, 235421 (2002).
[9] C. Bonet, D. Spence, and S. Tear, Surf. Sci. **504**, 183 (2002).
[10] E. Duverger, F. Palmino, E. Ehret, and J.-C. Labrune, Surf. Sci. **595**, 40 (2005).
[11] E. W. Perkins, C. Bonet, and S. P. Tear, Phys. Rev. B **72**, 195406 (2005).
[12] P. Wetzel, C. Pirri, P. Paki, D. Bolmont, and G. Gewinner, Phys. Rev. B **47**, 3677 (1993).
[13] M. Lohmeier, W. Huisman, E. Vileg, A. Nishiyama, and C. Nicklin, Surf. Sci. **345**, 247 (1996).
[14] L. Stauffer, A. Mharchi, C. Pirri, P. Wetzel, D. Bolmont, G. Gewinner, and C. Minot, Phys. Rev. B **47**, 10555 (1993).
[15] T. P. Roge, F. Palmino, C. Savall, J. C. Labrune, P. Wetzel, C. Pirri, and G. Gewinner, Phys. Rev. B **51**, 10998 (1995).
[16] P. Wetzel, S. Saintenoy, C. Pirri, D. Bolmont, G. Gewinner, T.

Roge, F. Palmino, C. Savall, and J. Labrune, Surf. Sci. **355**, 13 (1996).
[17] J. A. Martín-Gago, J. M. Gómez-Rodriguez, and J. Y. Veuillen, Phys. Rev. B **55**, 5136 (1997).
[18] C. Rogero, J. A. Martín-Gago, and J. I. Cerdá, Phys. Rev. B **74**, 121404(R) (2006).
[19] C. Rogero, C. Koitzsch, M. E. Gonzalez, P. Aebi, J. Cerdá, and J. A. Martín-Gago, Phys. Rev. B **69**, 045312 (2004).
[20] G. H. Cocoletzi, M. T. R. de la Cruz, and N. Takeuchi, Surf. Sci. **602**, 644 (2008).
[21] L. Magaud, A. Pasturel, G. Kresse, and J. Hafner, Phys. Rev. B **55**, 13479 (1997).
[22] G. W. Peng, Y. P. Feng, M. Bouville, D. Z. Chi, A. C. H. Huan, and D. J. Srolovitz, Phys. Rev. B **76**, 033303 (2007).
[23] M. D. Segall, P. J. D. Lindan, M. J. Probert, C. J. Pickard, P. J. Hasnip, S. J. Clark, and M. C. Payne, J. Phys.: Condens. Matter **14**, 2717 (2002).
[24] J. P. Perdew, K. Burke, and M. Ernzerhof, Phys. Rev. Lett. **77**, 3865 (1996).
[25] H. J. Monkhorst and J. D. Pack, Phys. Rev. B **13**, 5188 (1976).
[26] H. Kitayama, S. P. Tear, D. J. Spence, and T. Urano, Surf. Sci. **482-485**, 1481 (2001).
[27] D. J. Spence, S. P. Tear, T. C. Q. Noakes, and P. Bailey, Phys. Rev. B **61**, 5707 (2000).
[28] A. Pratt, A. Roskoss, H. Ménard, and M. Jacka, Rev. Sci. Instrum. **76**, 053102 (2005).
[29] A. L. Wachs, T. Miller, T. C. Hsieh, A. P. Shapiro, and T. C. Chiang, Phys. Rev. B **32**, 2326 (1985).
[30] J. Appelbaum and D. Hamann, Phys. Rev. Lett. **31**, 106 (1973).
[31] S. Saintenoy, P. Wetzel, C. Pirri, D. Bolmont, and G. Gewinner, Surf. Sci. **349**, 145 (1996).
[32] P. Wetzel, C. Pirri, and G. Gewinner, Europhys. Lett. **38**, 359 (1997).
[33] A. Pratt, C. Woffinden, C. Bonet, and S. Tear, Phys. Rev. B **78**, 155430 (2008).
[34] S. Masuda, H. Ishii, and Y. Harada, Solid State Commun. **82**, 587 (1992).
[35] Guo-Xin Qian and D. Chadi, J. Vac. Sci. Technol. A **5**, 906 (1987).
[36] S. Masuda, H. Ishii, and Y. Harada, Surf. Sci. **242**, 400 (1991).
[37] H. Ishii, S. Masuda, and Y. Harada, J. Electron Spectrosc. Relat. Phenom. **52**, 127 (1990).
[38] E. W. Perkins, I. M. Scott, and S. P. Tear, Surf. Sci. **578**, 80 (2005).
[39] C. Bonet, I. M. Scott, D. J. Spence, T. J. Wood, T. C. Q. Noakes, P. Bailey, and S. P. Tear, Phys. Rev. B **72**, 165407 (2005).
[40] D. J. Spence, T. C. Q. Noakes, P. Bailey, and S. P. Tear, Phys. Rev. B **62**, 5016 (2000).